

## Heavy carriers and non-Drude optical conductivity in MnSi

F. P. Mena,<sup>1</sup> D. van der Marel,<sup>1</sup> A. Damascelli,<sup>1</sup> M. Fäth,<sup>2</sup> A. A. Menovsky,<sup>2</sup> and J. A. Mydosh<sup>2,3</sup>

<sup>1</sup>Material Science Center, University of Groningen, 9747 AG Groningen, The Netherlands

<sup>2</sup>Kamerlingh Onnes Laboratory, Leiden University, 2500 RA Leiden, The Netherlands

<sup>3</sup>Max-Planck-Institute for Chemical Physics of Solids, D-01187 Dresden, Germany

(Received 10 April 2003; published 13 June 2003)

The optical properties of the weakly helimagnetic metal MnSi have been determined in the photon energy range from 2 meV to 4.5 eV using the combination of grazing incidence reflectance at 80° (from 2 meV to 0.8 eV) and ellipsometry (from 0.8 to 4.5 eV). As the sample is cooled below 100 K, the effective mass develops a strong frequency dependence at low frequencies, while the scattering rate develops a sublinear frequency dependence. The complex optical conductivity can be described by the phenomenological relation  $\sigma(\omega, T) \propto [\Gamma(T) + i\omega]^{-0.5}$ .

DOI: 10.1103/PhysRevB.67.241101

PACS number(s): 78.20.-e, 78.30.-j, 71.27.+a, 71.28.+d

The weakly helimagnetic metal MnSi ( $T_C = 29.5$  K) has been the subject of intensive studies during the last 40 years. In the helimagnetic phase, the resistivity has a  $T^2$  dependence, which has been explained as resulting from a coupling of the charge carriers to spin fluctuations.<sup>1</sup> Recently, interest has shifted to the quantum phase transition<sup>2</sup> at a critical pressure of 14.6 kbar, where the Curie temperature becomes zero. The temperature dependence of the resistivity outside the magnetically ordered region, at high pressures, has been found to be proportional to  $T^{3/2}$  in a temperature range far larger than that predicted by the so-called nearly ferromagnetic Fermi-liquid theory (an extension of the Fermi-liquid picture).<sup>2</sup> This fact has suggested the non-Fermi-liquid nature of MnSi in the normal state.<sup>2</sup> Despite these efforts in understanding the physics behind MnSi, few attempts have been made to determine and understand its optical properties. Measurements below  $T_C$  of the far infrared normal incidence reflectivity indicated a remarkable departure from the Hagen-Rubens law, usually observed in metals.<sup>3</sup> However, the high value of the reflection coefficient close to the 100% line prevented a detailed analysis of the frequency-dependent optical conductivity in this range. In this Rapid Communication, we overcome this hurdle by using  $p$ -polarized light at a grazing angle of incidence of 80°, for which the reflection coefficient drops well below the 100% line. We show that the frequency-dependent-scattering rate and the effective mass deviate from the behavior expected for Fermi liquids which can be understood from the fact that the optical conductivity is best described with an expression that departs from the usual Drude model.

Single crystals were grown using the traveling floating-zone technique.<sup>3,4</sup> The temperature dependence of the resistivity is shown in Fig. 1. Fitting the resistivity to  $\rho(T) = \rho(0) + AT^\mu$  in the temperature interval 4–23 K, we obtain  $\rho(0) = 1.85 \mu\Omega \text{ cm}$ ,  $A = 0.021 \mu\Omega \text{ cm K}^{-2}$ , and  $\mu = 2.1$ . The resistivity increases more rapidly in the region between 23 K and the phase transition. For  $T > 30$  K, the resistivity fits to  $\rho_p(T) = [1/\rho_\infty + 1/(\rho'T)]^{-1}$ , with  $\rho_\infty = 286 \mu\Omega \text{ cm}$  and  $\rho' = 1.62 \mu\Omega \text{ cm K}^{-1}$ . The remarkable accuracy of this parallel resistor formula<sup>5</sup> is further confirmed by the logarithmic derivative shown in the inset of Fig. 1. The tendency of the resistivity toward saturation at a value  $\rho_\infty$  for  $T \rightarrow \infty$  is in

agreement with Gunnarsson's result<sup>6</sup> that the resistivity saturates when the mean free path  $l = 0.5n^{1/3}d$  (roughly the Ioffe-Regel limit), where  $n$  is the density of the electrons and  $d$  is lattice parameter. Also, this indicates that if the temperature saturation would be absent, the resistivity would be proportional to  $T$  with a very high accuracy. These observations stand in stark contrast to the  $T^{5/3}$  temperature dependence predicted from the model of spin fluctuations in itinerant electron magnetism.<sup>1</sup>

Grazing incidence reflectivity was measured in the range 20–6000  $\text{cm}^{-1}$  using a Bruker 113v Fourier transform-infrared spectrometer [Figs. 2(a) and 2(b)]. The temperature dependence was measured using a home-built cryostat, the special construction of which guarantees the stable and temperature-independent optical alignment of the sample. The intensities were calibrated against a gold reference film evaporated *in situ* without repositioning or rotating the sample holder. In the range 20–100  $\text{cm}^{-1}$ , we measured the temperature dependence of the grazing reflectivity with 0.5

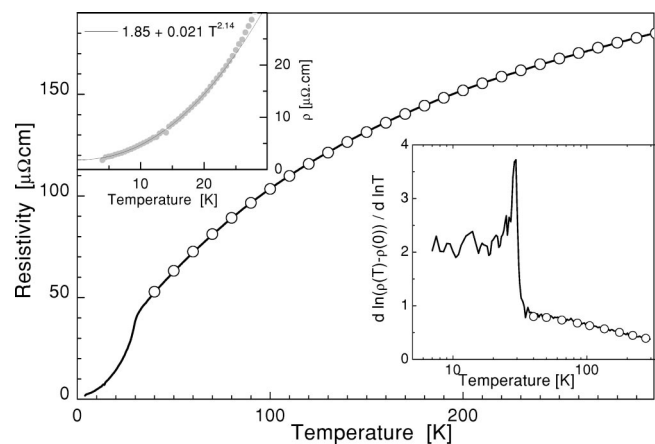


FIG. 1. dc resistivity as a function of temperature (solid curve). The open symbols represent  $\rho_p(T) = [1/\rho_\infty + 1/(\rho'T)]^{-1}$ , with  $\rho_\infty = 286 \mu\Omega \text{ cm}$  and  $A = 1.62 \mu\Omega \text{ cm K}^{-1}$ . Top left inset: dc resistivity below 30 K (dots) and fit to  $\rho_F(T) = \rho(0) + AT^\mu$ . Lower right inset: Temperature dependence  $\mu(T)$  of the exponent in  $\rho(T) = \rho(0) + AT^\mu$  (solid curve). The open symbols represent  $d \ln \rho_p / d \ln T$ .

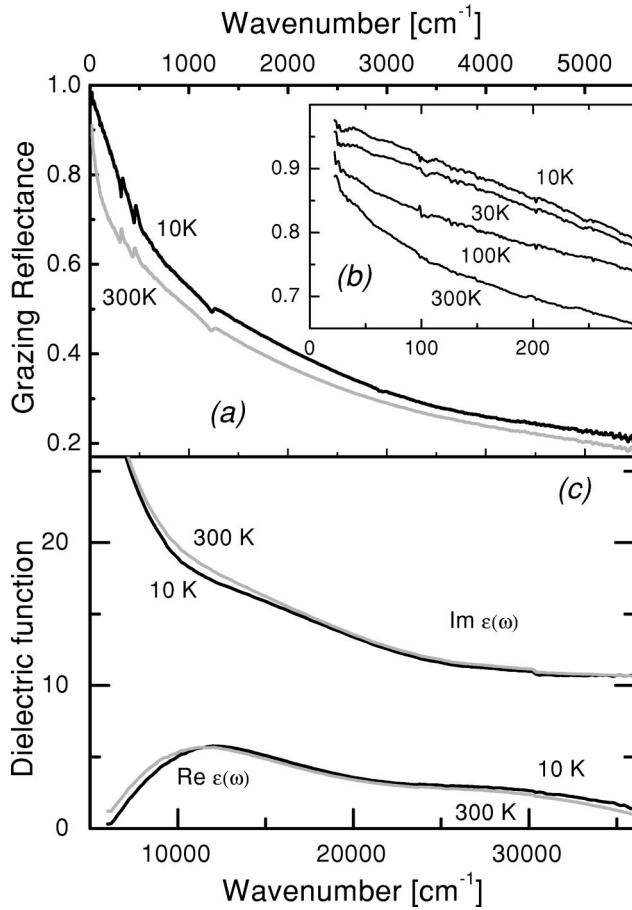


FIG. 2. (a) Grazing reflectivity at 10 and 300 K. (b) Expanded view of the reflectivity below 300 cm<sup>-1</sup>. (c) Real and imaginary parts of the dielectric function in the visible part of the spectrum measured with spectroscopic ellipsometry.

K intervals below 50 K and 2 K intervals above 50 K. The complex dielectric function in the range 6000–36 000 cm<sup>-1</sup> was measured with a commercial (Woollam VASE32) ellipsometric spectrometer for the same set of temperatures as the grazing reflectivities using an ultrahigh-vacuum cryostat [Fig. 2(c)]. The complex dielectric function  $\epsilon(\omega) = \epsilon'(\omega) + i(4\pi/\omega)\sigma_1(\omega)$  was calculated from the complete dataset (grazing infrared reflectance and visible ellipsometry) using Kramers-Kronig relations, following the procedure described in Ref. 7. Below 20 cm<sup>-1</sup>, the reflectivity data were extrapolated to fit the experimentally measured dc conductivities. The optical conductivity is shown for some temperatures in Fig. 3.

The first remarkable feature in the spectra is the similarity of the optical conductivity to the response of heavy fermion systems.<sup>8</sup> In these materials,  $\sigma(\omega)$  has almost no temperature dependence down to a frequency of  $\sim 10$  cm<sup>-1</sup> and, below this frequency, a narrow mode centered at zero frequency is formed.<sup>8</sup> A similar behavior has also been noticed for  $\alpha$  cerium<sup>7</sup> in the mid-infrared frequency range. Following a common procedure in the study of the electrodynamic response of heavy fermion systems, we have calculated  $1/\tau(\omega)$  and  $m^*(\omega)/m$  from the optical conductivity using the extended Drude model:<sup>9</sup>

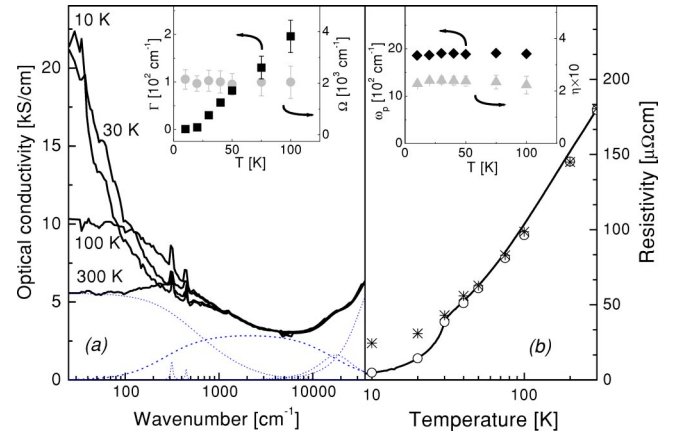


FIG. 3. (a) Optical conductivity at four different temperatures. (b) Measured dc resistivity, and dc resistivity obtained by extrapolating the experimental  $\sigma(\omega)$  using a Drude-Lorentz fit (stars) and using Eq. (4) (open circles). The fit parameters are presented in the insets.

$$\sigma(\omega) = \frac{\omega_p^2}{4\pi} \frac{1}{1/\tau(\omega) - i\omega m^*(\omega)/m} \quad (1)$$

adopting the value 18 700 cm<sup>-1</sup> for the plasma frequency, motivated by the least-square fits, which we will discuss below. Figure 4(a) indicates a significant mass renormalization at low frequencies which, at the lowest measured temperatures, shows no indication of reaching a frequency independent value. Previous de Haas–van Alphen experiments (at  $T=0.35$  K) (Ref. 10) provided an *average* enhancement of 4.5 times the cyclotron mass, although values as high as 14 were observed for some of the orbits. This average value was found to be compatible with the enhancement of the linear coefficient of the heat capacity  $\gamma/\gamma_0=5.2$  calculated from specific heat data of Ref. 11. In comparison, our data show at 10 K and at the lowest measured frequency an enhancement of 4, and an enhancement of 17 when we extrapolate the data to  $\omega=0$ .

The second remarkable feature is the behavior of  $1/\tau(\omega)$  [Fig. 4(b)]. At high temperatures, this quantity becomes frequency independent, as expected for a Drude peak. Already at 100 K,  $1/\tau(\omega)$  is no longer a constant. Approaching the phase transition,  $1/\tau(\omega)$  becomes strongly frequency dependent between 30 and 300 cm<sup>-1</sup>, and it follows approximately a linear frequency dependence in this frequency range. In contrast, other correlated systems, such as heavy fermions<sup>7,8</sup> and perovskite titanates,<sup>12</sup> show a frequency-dependent scattering rate with an  $\omega^2$  dependence at low frequencies. Indeed, the theory of Fermi liquids<sup>13</sup> predicts

$$1/\tau(\omega, T) = 1/\tau_0 + a(\hbar\omega)^2 + b(k_B T)^2 \quad (2)$$

with  $b/a = \pi^2$ . The same expression was obtained by Millis and Lee considering the Anderson lattice model,<sup>14</sup> and qualitatively similar behavior has been calculated by Riseborough in the context of spin fluctuations (with  $b/a = 4\pi^2$ ).<sup>15</sup> The corresponding frequency dependence of  $1/\tau(\omega)$  is plotted in the inset of the lower panel of Fig. 4 for 10 K. There is a

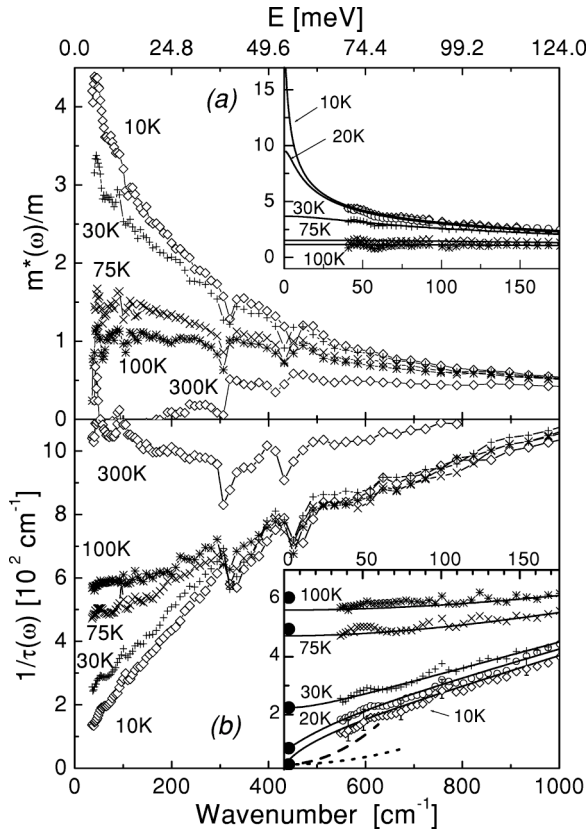


FIG. 4. (a) Effective mass and (b) frequency-dependent scattering rate in MnSi as obtained from  $\sigma(\omega)$  at different temperatures (Insets: Same quantities below  $200 \text{ cm}^{-1}$ ). Symbols represent the experimental data and thick lines the calculation from the non-Drude fit described in the text. The solid points at the left show  $\rho_{DC}\omega_p^2/(4\pi)$ . The inset of the lower panel shows also the expected frequency dependence for the Fermi-liquid theory (dashed line) and spin fluctuations (dotted line) calculated from Eq. (2).

mismatch with the experimental  $1/\tau(\omega)$ , both in the absolute value and in the observed trend, which is outside the experimental errorbars. However, it cannot be excluded that at an even lower frequency, the experimental  $1/\tau(\omega)$  would cross over to an  $\omega^2$  dependence.

Above, we have pointed out various striking results in the optical response of MnSi. In order to understand their nature, let us take a closer look at the low-frequency data. From 300 to 75 K,  $1 - R_p(\omega)$  follows an  $\omega^{1/2}$  behavior [see Fig. 2(b)]. This can easily be understood from the fact that at low frequencies, from the Fresnel formulas,  $R_p$  can be written approximately as

$$R_p = 1 - \frac{2\omega^{1/2}}{\cos\theta} \operatorname{Re} \left[ \frac{1}{\sqrt{i\pi\sigma(\omega)}} \right], \quad (3)$$

where  $\theta$  is the angle of incidence. In the case where  $\sigma_1$  is constant and  $\sigma_2$  goes to zero, this expression reduces to the well-known Hagen-Rubens law. In the Drude picture, this corresponds to the frequency range where the scattering rate is larger than  $\omega$ . In contrast, below 75 K, our measured  $R_p$  does not follow an  $\omega^{1/2}$  behavior. Combining the Drude

model with the Fresnel equations for reflectivity, a plateau in the reflectivity is expected for *intermediate* frequencies (frequencies larger than the scattering rate but much lower than the plasma frequency). To check this more closely, we measured  $R_p$  below  $100 \text{ cm}^{-1}$  in a finer temperature mesh. Our results show no sign of a plateau, instead  $1 - R_p(\omega)$  evolves gradually to a linear frequency dependence when  $T$  is lowered. We can then conclude that either the peak centered at zero frequency departs from the Drude picture or other modes appear at low temperatures and at low frequencies. To distinguish between these alternatives, we have fitted, simultaneously, the measured reflectivity, ellipsometry, and resistivity with two models. First, we modeled the data with a Drude peak and a set of oscillators. In this case, the fit fails to reproduce the measured dc resistivities at low temperatures [stars in Fig. 3(b)]. On the other hand, if we give more fitting weight to  $\rho_{DC}$ , the result is a poor fit of  $R_p$  at low frequencies. Indeed, the infrared properties together with the dc resistivity can be summarized in an economical way (i.e., requiring a minimal set of adjustable parameters) when we replace the Drude formula with<sup>16</sup>

$$\sigma(\omega) = \frac{\omega_p^2}{4\pi} \frac{i}{(\omega + i\Gamma)^{1-2\eta} (\omega + i\Omega)^{2\eta}}, \quad (4)$$

which for  $\Gamma \ll \omega \ll \Omega$  corresponds to the expression derived by Anderson in the context of the optical conductivity of the cuprate high- $T_c$  superconductors,  $\sigma(\omega) \propto (i\omega)^{2\eta-1}$ .<sup>16,17</sup> Equation (4), in the case  $\Omega \gg \omega$ , has been shown to describe the optical conductivity of SrRuO<sub>3</sub>, below 40 K, in the range  $6 - 2400 \text{ cm}^{-1}$  with  $\eta = 0.3$ .<sup>18</sup> For SrRuO<sub>3</sub>, this behavior has been justified as arising from the coupling of electrons to orbital degrees of freedom,<sup>19</sup> and in the context of the discrete filamentary model of charge transport.<sup>20</sup>

Our new fit, non-Drude plus Lorentz oscillators [whose individual components at 300 K are displayed in Fig. 3(a)], gives the same overall result at high temperatures ( $T > 75 \text{ K}$ ) as the Drude fit. However, at low temperatures, the non-Drude equation gives a better fit at low frequencies and, what is more important, reproduces  $\rho_{DC}$  at all temperatures [open symbols in Fig. 3(b)]. Therefore, we conclude that the low-frequency optical response of MnSi is best described by Eq. (4). From the fit, we can extrapolate the optical properties to lower frequencies (insets of Fig. 4). The extrapolation shows that at 10 K, for  $\omega \rightarrow 0$ ,  $m^*(\omega)/m = 17$ , with a gradual decay as a function of increasing frequency. Similarly,  $1/\tau(\omega)$  is approximately proportional to  $\omega$  in the frequency range below  $300 \text{ cm}^{-1}$ . Above  $T_C$ , it has a weak  $\omega^2$  frequency dependence.

Now let us analyze the parameters of the fit to Eq. (4), which are summarized in the insets of Fig. 3 (the errorbars represent the interval of confidence calculated for a variation of 1% of  $\chi^2$ ). Within the errorbars, the parameters  $\omega_p$ ,  $\Omega$ , and  $\eta$  are temperature independent, which contrasts with the strong temperature dependence of  $\Gamma$ . From Eq. (4), we can easily see that  $\rho_{DC} = 4\pi\omega_p^{-2}\Omega^{2\eta}\Gamma^{1-2\eta}$ , but since  $\omega_p$ ,  $\Omega$ , and  $\eta$  are temperature independent,  $\rho_{DC}(T) \propto \Gamma(T)^{1-2\eta}$ . For our sample, using the values of Fig. 3, we obtain  $\rho_{DC} = 6.02\Gamma^{0.54} \mu\Omega \text{ cm}$ . Recently, Dodge *et al.*<sup>18</sup> have empha-

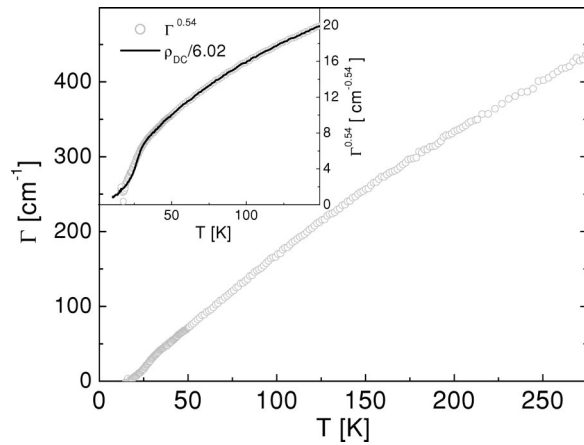


FIG. 5. Temperature dependence of  $\Gamma$  (see text). *Inset*: Temperature dependence of  $\Gamma^{0.54}$  (circles) and of  $\rho_{DC}\omega_p^2/(4\pi\Omega^{2\eta})$  (solid line).

sized a similar nonlinear relationship between the dc resistivity and the parameter  $\Gamma$  in the case of the weak itinerant ferromagnet SrRuO<sub>3</sub>. The conclusions for SrRuO<sub>3</sub> have been questioned recently by Capogna *et al.*,<sup>21</sup> who argued that the true temperature dependence of the optical properties may have been masked by the large residual resistivity of the sample used in Ref. 18. In the present work, this problem is absent due to the low residual resistivity of single crystalline MnSi. In fact, we can confirm this nonlinear relation *independently* by fitting the low frequency  $R_p$  (at all the measured temperatures) to Eq. (4) using the known values of  $\omega_p$ ,  $\Omega$ , and  $\eta$ . The values obtained for  $\Gamma$  are displayed in Fig. 5. The inset shows  $\Gamma^{0.54}$  and  $\rho_{DC}/6.02$ . We can see that the model represented by Eq. (4) describes the measured data (reflectivity and resistivity) down to  $\approx 20$  K.

At low frequencies, deviations from the Drude formula of the optical conductivity have been seen accompanied by de-

viations from  $T^2$  in  $\rho_{DC}$  [for example, YBCO (Ref. 22) and CaRuO<sub>3</sub> (Ref. 23)]. Therefore, a departure from Drude behavior has been usually considered as a evidence against the Fermi-liquid behavior. Here, for MnSi, we are confronted with an atypical case. The resistivity has a quadratic temperature dependence, but the optical conductivity is better described by Eq. (4) with  $\eta \approx 0.2$ , a clear departure from the Drude formulation. Moreover, instead of an  $\omega^2$ -type frequency-dependent-scattering rate, which is usually observed in strongly interacting Fermi liquids,<sup>7,8</sup> here  $1/\tau(\omega)$  has a sublinear frequency dependence. Although Eq. (4) summarizes in a compact way the low-frequency optical response, differing in a fundamental way from conventional Drude behavior, its microscopic origin is as yet not fully understood.

For frequencies below  $300 \text{ cm}^{-1}$  and for  $T < 100$  K, the situation can be summarized as follows.

(i)  $m^*/m$  decreases from 17 to 1 as temperature and frequency are increased.

(ii) Phenomenologically the dc conductivity and the optical conductivity follow  $\sigma \propto (\Gamma(T) + i\omega)^{-0.5}$ . In this formulation  $\Gamma(T) \propto T^4$  below  $T_C$ , whereas above  $T_c$  the temperature dependence is approximately linear.

(iii) For  $T > T_C$ , the scattering rate  $1/\tau(\omega, T)$  is proportional to  $T$  and  $\omega^2$  in contradiction with the theory of weak itinerant ferromagnetism.

(iv) For  $T < T_C$ , the scattering rate is proportional to  $T^2$  and  $\omega$ . Given the frequency range for this type of measurements, we can not exclude the possibility that for frequencies below  $30 \text{ cm}^{-1}$ , the scattering rate crosses over to the Fermi-liquid result  $1/\tau \propto \pi^2 T^2 + \omega^2$ .

This project is supported by the Netherlands Foundation for Fundamental Research on Matter with financial aid from the Nederlandse Organisatie voor Wetenschappelijk Onderzoek.

<sup>1</sup>T. Moriya, *Spin Fluctuations in Itinerant Electron Magnetism* (Springer, Berlin, 1985).

<sup>2</sup>C. Pfleiderer, S.R. Julian, and G.G. Lonzarich, *Nature* (London) **414**, 427 (2001).

<sup>3</sup>A. Damascelli, Ph.D. Thesis, University of Groningen, The Netherlands, 1999.

<sup>4</sup>M. F ath, Ph.D. Thesis, University of Leiden, The Netherlands, 1999.

<sup>5</sup>H. Wiesmann *et al.*, *Phys. Rev. Lett.* **38**, 782 (1977).

<sup>6</sup>M. Calandra and O. Gunnarsson, *Phys. Rev. B* **66**, 205105 (2002).

<sup>7</sup>J.W. van der Eb *et al.*, *Phys. Rev. Lett.* **86**, 3407 (2001).

<sup>8</sup>L. Degiorgi, *Rev. Mod. Phys.* **71**, 687 (1999).

<sup>9</sup>J.W. Allen and J.C. Mikkelsen, *Phys. Rev. B* **15**, 2952 (1977).

<sup>10</sup>L. Taillefer *et al.*, *J. Magn. Magn. Mater.* **54-57**, 957 (1986).

<sup>11</sup>E. Fawcett *et al.*, *Int. J. Magn.* **1**, 29 (1970).

<sup>12</sup>T. Katsufuji and Y. Tokura, *Phys. Rev. B* **60**, 7673 (1999).

<sup>13</sup>D. Pines and P. Nozi ers, *The Quantum Theory of Solids* (Benjamin, New York, 1966).

<sup>14</sup>A.J. Millis and P.A. Lee, *Phys. Rev. B* **35**, 3394 (1987).

<sup>15</sup>P.S. Riseborough, *Phys. Rev. B* **27**, 5775 (1983).

<sup>16</sup>D. van der Marel, *Phys. Rev. B* **60**, R765 (1999).

<sup>17</sup>P.W. Anderson, *Phys. Rev. B* **55**, 11 785 (1997).

<sup>18</sup>J.S. Dodge *et al.*, *Phys. Rev. Lett.* **85**, 4932 (2000). The exponent  $\eta$  in this paper is related to the exponent  $\alpha$  of Dodge *et al.* by  $\alpha = 1 - 2\eta$ .

<sup>19</sup>M.S. Laad and E. M uller-Hartmann, *Phys. Rev. Lett.* **87**, 246402 (2001).

<sup>20</sup>J.C. Phillips, *Philos. Mag. B* **81**, 757 (2001).

<sup>21</sup>L. Capogna *et al.*, *Phys. Rev. Lett.* **88**, 076602 (2002).

<sup>22</sup>Z. Schlesinger *et al.*, *Phys. Rev. Lett.* **65**, 801 (1990).

<sup>23</sup>Y.S. Lee *et al.*, *Phys. Rev. B* **66**, 041104(R) (2002).